Supporting Information

Giraud et al. 10.1073/pnas.0910627107

SI Materials and Methods

Induction of Active EAE and Hormone Treatment. Chronic EAE was induced with myelin oligodendrocyte glycoprotein (MOG)35–55 peptide in C57BL/6 female mice (9–10 weeks old; Harlan) immunized with $MOG_{35–55}$, complete Freund's adjuvant (CFA), and pertussis toxin. This model leads to ascending limb paralysis, with spinal cord white matter inflammatory lesions, gliosis, axonal damage, and demyelination (1, 2). Motor impairment was scored daily for clinical disease severity according to the 0–5 EAE grading scale (2). On day postimmunization (dpi) 14 corresponding to score 1.5–2, EAE mice were implanted with 17β-estradiol (E2, 5 mg s.c./21-day release to raise E2 levels to pregnancy levels, n = 13) or placebo (n = 14) pellets (Innovative Research of America) under light ketamine/xylazine anesthesia. Control mice receiving PBS/CFA emulsion, pertussis toxin, and placebo pellets did not develop EAE. We also checked that a low-dose E2 implant (0.1 mg, to maintain estrus levels ∼0.3–0.7 nM) performed after disease onset in seven mice did not affect EAE clinical course, in agreement with previous reports. Animals were killed at 28–30 dpi with lethal anesthesia. After atrium cut, blood was collected in EDTA-coated microvettes (Sarstedt) for plasma estradiol measurements (seven mice/group). Fresh lumbar spinal cords (six mice/group) were also frozen on dry ice and kept at −80 °C until RNA extraction and multiplex qPCR.

Enzyme Immunoassays. 17β-estradiol was measured from plasma samples after ethyl ether extraction according to manufacturer's instructions (Oxford Biomedical Research). CCL2 content in culture media was quantified using a rat OptiEIA ELISA Set (BD Biosciences) or a mouse Quantikine ELISA Kit (R&D).

Immunohistochemistry on Mouse Spinal Cord. Three mice per group (controls, EAE, and EAE + E2) were deeply anesthetized and perfused transcardially with ice-cold 0.9% saline, followed by 4% paraformaldehyde in phosphate buffer solution (PFA). Lumbar spinal cords were removed, postfixed in PFA, and cryoprotected with 20% sucrose solution in 0.01 M PBS (pH 7.3) and frozen in cold isopentane. Cryostat sections (16 μm thick) were cut coronally and collected serially on Superfrost plus slides, with control, EAE, and EAE + E2 sections on the same slide. Sections were treated with 0.3% H_2O_2 and 0.1% sodium azide in PBS for 30 min followed by 30% normal donkey serum and 0.05–0.1% Triton X-100 in PBS for 30 min. Rat anti-GFAP (1:200; Zymed/Invitrogen) and rat anti-mouse CD45 (1:200; BD Pharmingen) were used for identification of astrocytes and infiltrating leukocytic cells, respectively. After overnight incubation at 4 °C, sections were rinsed and incubated 1 h at room temperature with appropriate Texas Red- or Rhodamine X-coupled F(ab′)2 secondary antibodies (1:200; Jackson ImmunoResearch), followed by PBS rinses. They were then incubated overnight with rabbit anti-CCL2 (1:2,000; Torrey-Pines), anti-osteopontin (1:100; Assays Designs), anti-ERα (polyclonal C1355, catalog no. 06-935, 1:4,000 or monoclonal 60C, catalog no. 05-820, 1:2,000; Upstate), or anti-ERβ (clone 68-4, catalog no. 05-824, 1:2,000; Upstate) diluted in 3% normal donkey serum and 0.05–0.1% Triton X-100 at 4 °C. [This rabbit clone is directed against an N-ter epitope that has been previously demonstrated to provide very good specificity for ERβ on brain sections (3). As an additional control experiment, we also tested another antibody directed against a C-ter epitope (affinity-purified rabbit polyclonal PA1-310; Thermo Scientific) that was initially well characterized on rodent brain sections by Alves et al. (4) and obtained spinal cord immunostainings similar to those with clone 68-4.] The sections were then rinsed for 45 min in phosphate buffer followed by incubation with biotinylated secondary anti-rabbit F(ab′)2 antibody (1:200; Jackson ImmunoResearch) for 45 min. Sections were incubated with streptavidin–peroxidase complex (Perkin-Elmer Life Sciences) at 1:200 for 1 h, rinsed, and incubated with tyramide–fluorescein solution (1:100 dilution; PerkinElmer Life Sciences) for 10 min at room temperature. Sections were incubated with DAPI at 1 μg/mL for 5 min, rinsed, and coverslipped with anti-fading mounting medium (Mowiol). Negative controls were treated as described above except that primary antibodies were omitted. Spinal cord sections were analyzed on a fluorescent microscope using appropriate filters (BX61; Olympus) and pictures were taken at ×5 to ×40 magnification using a digital camera (DP 50; Olympus) connected to an image-acquisition software (Analysis; Olympus). The average gray level of immunofluorescence for CCL2 or GFAP was measured in the gray matter (dorsal horn and ventral horn) and the white matter (ventral, dorsal, and lateral funiculi) from ×10 fields with ImageJ software, substracted from the corresponding background (no primary antibody), and expressed as relative to the signal in the dorsal horn of control animals. The number of CD45-IR cells and of ERα-IR or ERβ-IR nuclei in the white matter was counted at ×40 magnification under the microscope (one field for ventral or dorsal funiculus and eight fields for lateral funiculus per section; three mice/group). For image presentation, brightness and contrast were adjusted with identical settings between treatments.

Confocal Laser Scanning Microscopy. Confocal images were acquired on a Leica SP2 AOBS microscope (Wetzlar). The slides were viewed with a ×63 magnification, 1.4 numerical aperture oil immersion objective. All fluorescent images (1,024 × 1,024 pixels) were generated using sequential laser scanning (400 Hz) with the corresponding single wavelength laser line (405, 488, or 543 nm) with pinhole set to one airy unit. Laser 543 nm at 50% of power and emission filter set at 555–650 nm were used to examine Rhodamine X staining. Laser 488 nm at 25% of power and emission filter set at 500–545 nm were used to examine FITC staining. DAPI staining was examined with laser 405 at 25% of power and emission filter set at 410–480 nm. Zoomed sections corresponding to the center of the cells are presented. No fluorescence was detected in absence of the primary antibody. Images from the same z series were collected using the same values for laser power and photomultiplier gain. Four scans were averaged per z section and 10 z sections were collected at 1-μm increments. Care was taken to ensure that pixel saturation was <10%. Acquired images were imported into ImageJ software (National Institutes of Health; http://rsb.info.nih.gov/ij/) and into Adobe Photoshop for image presentation.

Cell Cultures and Treatments. Astrocytes were cultured according to the protocol developed by McCarthy and deVellis (5) with some modifications. Wistar rat or C57BL/6 mouse pups (1–3 days old) were cold anesthetized and decapitated, the hemispheres or spinal cords were removed, and the meninges discarded. Spinal cords from C57BL/6 female adult mice were also removed after cervical dislocation. After trypsin/DNase treatment, the tissues were dissociated mechanically and cells passed through a cell strainer (70 μm). After centrifugation, the cells were resuspended in culture medium containing DMEM (high glucose DMEM), Glutamax, nonessential amino acids, 1 mM pyruvate

sodium, 1% penicillin/streptomycin, and 10% FBS (Invitrogen) and then plated in 75-cm^2 flasks and incubated at 37 °C in a humid atmosphere with 5% CO_2. The medium was changed twice weekly. When cultures became confluent (2 weeks), the flasks were shaken at 225 rpm during 4 h at 37 °C to dislodge microglia and oligoprecursors. The astrocyte-enriched layer was passaged into new flasks. When flasks became confluent again, cells were subcultured in poly-D-lysine-coated culture plates for experiments. The cultures consist of >99% astrocytes as determined by immunoreactivity for GFAP. All experiments were carried out when the subcultures had become near to confluence. Propyl pyrazole triol (PPT, ERα agonist) and 2,3-bis(4-hydroxyphenyl) proprionitrile (DPN, ERβ agonist) or ICI 182,170 were from Tocris. 17β-estradiol (E2), 17α-estradiol, and E2-BSA were purchased from Sigma Chemical. Recombinant cytokines were provided by Biosource or AbD Serotec. Astrocytes were switched to serum- and phenol red-free DMEM overnight before treatments. For evaluation of the effects of estrogen, astrocytes were pretreated with E2 or vehicle for 30 min, followed by TNFα (10 ng/mL) or vehicle for 30 min (p65 translocation study), and for 6–8 or 16–18 h (RNA or protein expression studies, respectively).

Luciferase Assay. Mouse neonatal spinal cord astrocytes cultured into 12-well plates for 24 h were lipofected with a Gaussia luciferase NFκB reporter plasmid (250 ng, pRR-high NFκB, Active motif). After overnight recovery and serum deprivation, cells were treated with or without E2 for 30 min, followed by a 2-h incubation in the presence or the absence of TNFα. Cell extracts were assayed for luciferase activity following manufacturer's instructions.

In Vitro Immunocytochemical Analysis. Treated astrocytes or microglia were fixed for 20 min with 4% paraformaldehyde in PBS at room temperature. Cells were rinsed three times with PBS and processed for GFAP or CD45 immunofluorescence followed by rabbit anti-CCL2, anti-ER, or anti-p65 (1:100; Santa Cruz) and tyramide–fluorescein detection, followed by DAPI staining as described above. For CCL2 expression in neonatal cortical astrocytes, the relative intensity of FITC fluorescence in acquired (unsaturated) images at ×40 magnification was measured using the histogram function after a threshold setting at 50, divided by the number of DAPI stained nuclei. For semiquantitative analysis of p65 localization, the percentage of immunolabeled nuclei in 100 postnatal cortical astrocytes/dish was calculated. The experiment was repeated with mouse neonatal and adult spinal cord astrocytes. For comparison, the experiment was conducted in parallel on microglia. Dislodged microglia from neonatal spinal cord cultures were seeded on uncoated 35-mm dishes for 2 h, and the medium was then replaced with DMEM with 5% FBS and 50% astrocyte conditioned medium for 3 days, followed by overnight serum deprivation, and treated with or without 10 nM E2 for 30 min followed by 30 min treatment with 10 ng/mL TNFα. Cultures were then processed for CD45 and p65 immunocytochemistry.

Quantitative Real-Time PCR. Total RNA was extracted from spinal cord tissues or from cell cultures using extraction kits (Macherey-Nagel). Following DNase and reverse transcriptase reaction, multiplex qPCR for CCL2 or osteopontin with α-tubulin as reference was analyzed on a 7000 real-time PCR system (ABI). The primers designed using Lux Primer software (Invitrogen) are rat and mouse gene specific confirmed by BLAST search. Amplified fragments cover regions 246–331 (exons 2–3) of CCL2 cDNA (GenBank accession no. AF_058786), 369–500 (exon 6) of osteopontin cDNA (NM_009263), and 1,003–1,073 (exon 4) of α-tubulin cDNA (NM_011654) as reference. After the final cycle of the PCR, a melt curve analysis was routinely performed. The respective Tm's were 80.5 °C for CCL2, 80 °C for osteopontin, and 82 °C for α-tubulin. To assess amplification efficiencies of target gene and α-tubulin, standard curves were generated with serial dilutions of total cDNA (300–1.5 ng). The slope approximates 3.4 for CCL2, 3.5 for osteopontin, and 3.3–3.4 for α-tubulin, indicating efficiency of the PCR. Quantification was performed in duplicates from 50 ng cDNA using the $2^{-\Delta\Delta Ct}$ method.

For ChIP analysis, mouse primers that amplify the 301-bp fragment containing the kB1 and kB2 binding sites in the TNFα-dependent enhancer region of the *CCL2* gene (6) were used. Treated cells (three 75-cm^2 flasks/group) were subjected to formaldehyde fixation and chromatin extraction according to the AdemChIP kit (Ademtech). After DNA shearing via sonication, aliquots were kept for input DNA as control reference or subjected to ChIP with 1 μg of either the rabbit p65 antibody or rabbit control IgG (mock). After decross-linking and DNA purification, qPCR was performed with SYBR-GreenER (Invitrogen) and amounts of PCR product from input DNA and ChIP samples were quantitated against a standard curve derived from serially diluted DNA (slope 3.5). The melt curves of PCR reactions from anti-p65 ChIP samples or input DNA indicated a peak at 81.7–82 °C corresponding to the 301-bp fragment.

1. Gold R, Linington C, Lassmann H (2006) Understanding pathogenesis and therapy of multiple sclerosis via animal models: 70 years of merits and culprits in experimental autoimmune encephalomyelitis research. *Brain* 129:1953–1971.
2. Nicot A, Kurnellas M, Elkabes S (2005) Temporal pattern of plasma membrane calcium ATPase 2 expression in the spinal cord correlates with the course of clinical symptoms in two rodent models of autoimmune encephalomyelitis. *Eur J Neurosci* 21:2660–2670.
3. Mitra SW, et al. (2003) Immunolocalization of estrogen receptor beta in the mouse brain: Comparison with estrogen receptor alpha. *Endocrinology* 144:2055–2067.
4. Alves SE, Lopez V, McEwen BS, Weiland NG (1998) Differential colocalization of estrogen receptor beta (ERbeta) with oxytocin and vasopressin in the paraventricular and supraoptic nuclei of the female rat brain: An immunocytochemical study. *Proc Natl Acad Sci USA* 95:3281–3286.
5. McCarthy KD, de Vellis J (1980) Preparation of separate astroglial and oligodendroglial cell cultures from rat cerebral tissue. *J Cell Biol* 85:890–902.
6. Boekhoudt GH, Guo Z, Beresford GW, Boss JM (2003) Communication between NF-kappa B and Sp1 controls histone acetylation within the proximal promoter of the monocyte chemoattractant protein 1 gene. *J Immunol* 170:4139–4147.

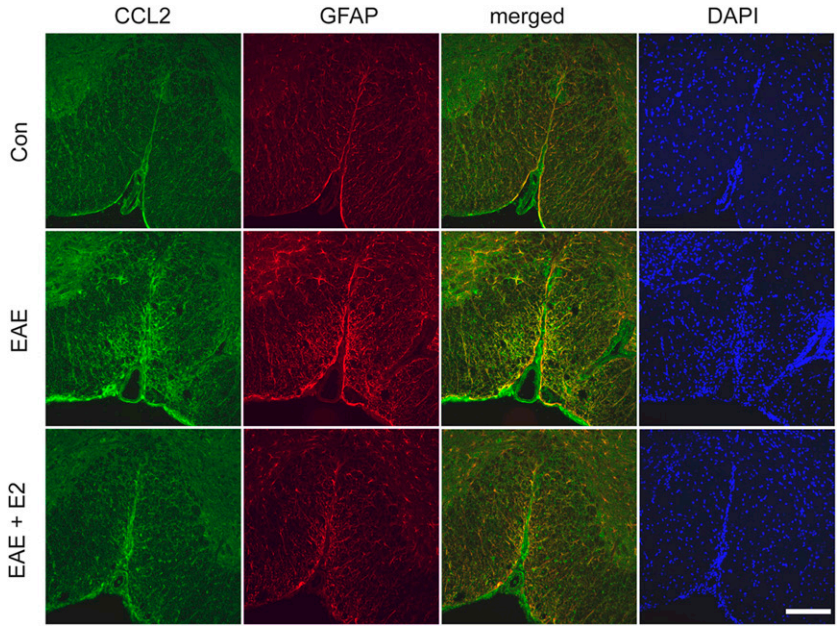

Fig. S1. Immunohistochemistry for CCL2 with the GFAP astrocytic marker in the ventral funiculus of placebo-treated control mice (Con), placebo-treated EAE mice (EAE), and E2 (5 mg)-treated EAE mice (EAE + E2). Labeling at ×20 magnification of CCL2 (green), GFAP (red), merged, and corresponding DAPI stainings is shown. (Scale bar, 160 μm.)

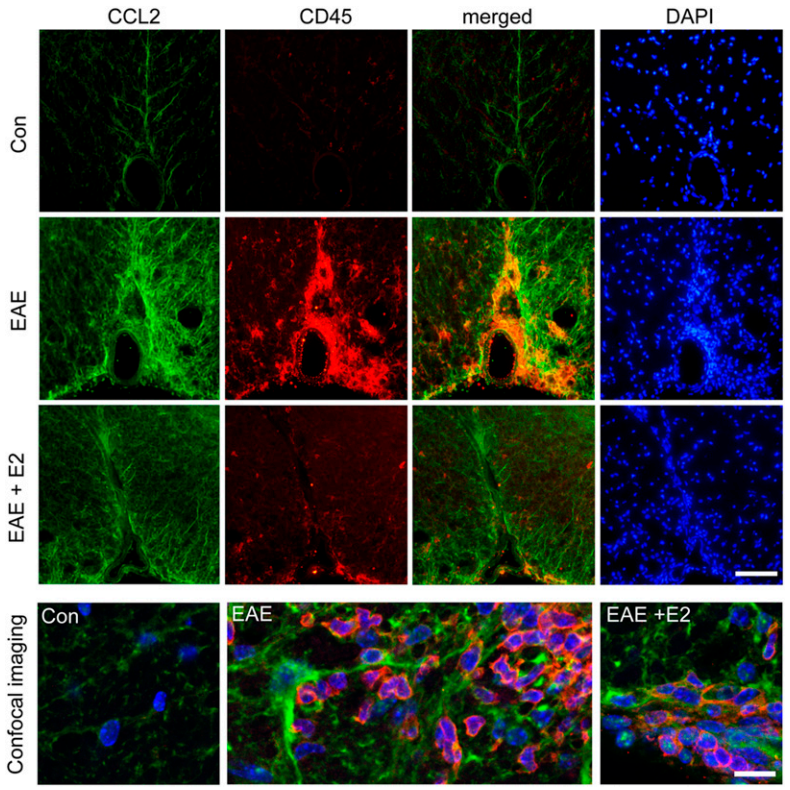

Fig. S2. Immunohistochemical analysis of CCL2 with the CD45 leukocytic marker in the ventral funiculus of placebo-treated control mice (Con), placebo-treated EAE mice (EAE), and E2 (5 mg)-treated EAE mice (EAE + E2). (*Upper*) Labeling at ×20 magnification of CCL2 (green), CD45 (red), merged, and corresponding DAPI stainings. (Scale bar, 160 μm.) (*Lower*) Confocal imaging (single confocal sections) of CCL2 and CD45 immunoreactivity with DAPI staining in control, EAE, and EAE + E2 ventral white matter. (Scale bar, 13 μm.)

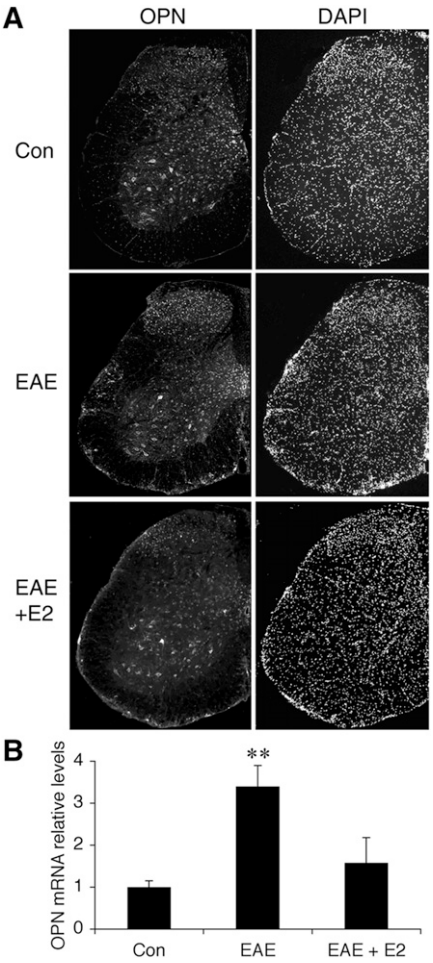

Fig. S3. Immunoreactivity for osteopontin (OPN) and corresponding DAPI staining on hemisections of control, EAE, and EAE + E2 spinal cords. For pictures of whole hemisections from ×5 objective, corner areas outside the spinal cord have been filled because of rotation of the initial pictures and presence of occasional nerve remainings. In controls (Con), OPN was mainly expressed in neuronal cell bodies in the gray matter. Increased OPN immunoreactivity in the white matter of placebo-treated EAE spinal cord correlated with areas of cellular infiltrates. In E2-treated EAE mice, OPN immunoreactivity was decreased in the white matter, remaining in smaller areas of infiltrating cells restricted around leptomeninges. (*B*) qPCR of OPN mRNA from spinal cord extracts. ANOVA, $F_{2,17} = 8.8$, $P < 0.005$; post hoc analysis, difference vs. controls, **, $P < 0.01$.

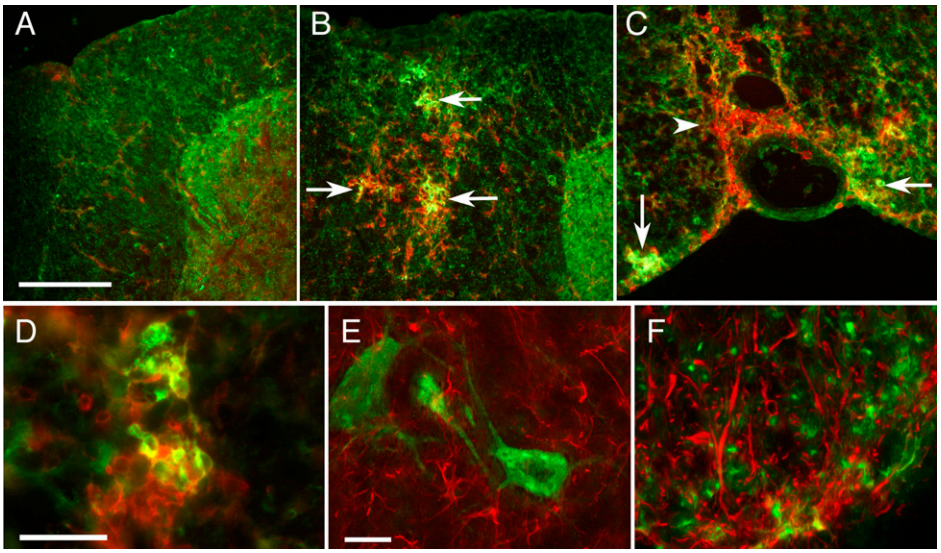

Fig. S4. Increased osteopontin immunoreactivity in the spinal cord of EAE mice. (*A*–*C*) Double immunofluorescence for osteopontin (green) and CD45 (red) in the dorsal spinal cord of a control mouse (*A*) and in the dorsal (*B*) or ventral (*C*) funiculus of an EAE mouse. Arrows, foci of parenchymal inflammation. Arrowhead, perivascular infiltrate not stained for osteopontin. (Scale bar, 150 μm.) (*D*) High magnification showing colocalization of osteopontin with CD45 in some infiltrating cells. (Scale bar, 50 μm.) (*E* and *F*) Double immunofluorescence for osteopontin (green) and GFAP (red) in the ventral gray matter (*E*) or white matter (*F*) of an EAE mouse. Osteopontin was present within motoneurons in the gray matter in control and EAE mice and was not associated with GFAP elements. In the EAE white matter, the elevated osteopontin labeling is not colocalized to GFAP immunoreactive fibers. (Scale bar, 50 μm.)

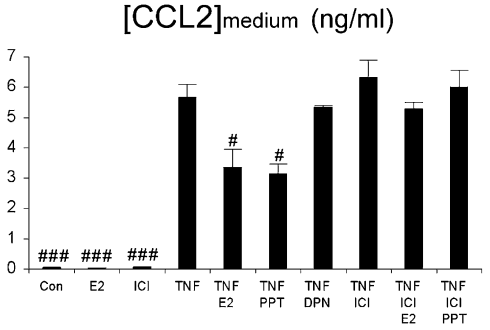

Fig. S5. Effects of 17β-estradiol and ERα or ERβ selective ligands on TNFα-induced CCL2 content in the medium of mouse neonatal spinal cord cultures. E2 and the ERα selective agonist PPT inhibit TNFα-induced CCL2 content. These effects are blocked by the ER antagonist ICI 182,170. In contrast, the ERβ selective agonist DPN had no effect on TNFα-induced CCL2 content. Con, control; DPN, 2,3-bis(4-hydroxyphenyl) proprionitrile (30 nM); E2, 17β-estradiol (30 nM); PPT, propyl pyrazole triol ERα selective agonist (30 nM); TNF, TNFα (10 ng/mL); ICI, ERα/β antagonist ICI 182,170 (5 μM). ICI (or vehicle) was added to cultures 1 h before estrogen treatments. Cells were incubated with TNFα (or PBS for Con, E2 alone, and ICI alone) for 17 h before medium collection and CCL2 Enzyme ImmunoAssay. Statistical analysis: ANOVA, $F_{9,39} = 49.1$, $P < 0.0001$, $n = 4$–5/group (two experiments). Difference vs. TNFα: #, $P < 0.05$; ###, $P < 0.001$.

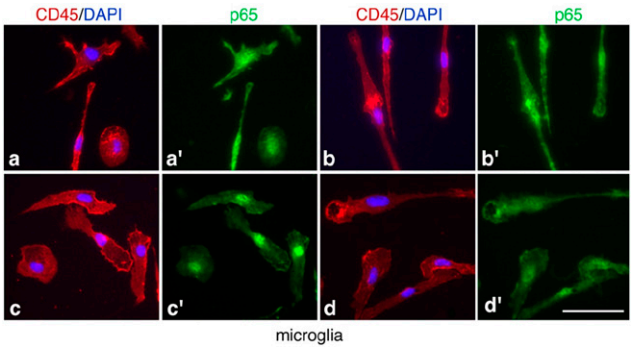

Fig. S6. Estradiol impedes TNFα-induced p65 nuclear translocation in cultured microglia. p65 immunoreactivity (green) in microglia stained for CD45 (red) and DAPI (blue) is shown. (Scale bar, 50 μm.) (*a* and *a*′) Controls; (*b* and *b*′) E2, 10 nM; (*c* and *c*′) TNFα, 10 ng/mL; (*d* and *d*′) TNFα + E2.

Table S1. Assessment of 17β-estradiol (E2) implant (5 mg) effectiveness

	Uterine weight[†]		
	Mean ± SEM	Minimum	Maximum
Con	90 ± 12	25	175
EAE + placebo	43 ± 6**	20	110
EAE + E2	175 ± 20***	100	220
	E2 plasma levels (pg/mL)[‡]		
	Mean ± SEM	Minimum	Maximum
Con	55 ± 14	34	138
EAE + placebo	46 ± 9	25	93
EAE + E2	1,622 ± 160***	1,131	2,218

Differences vs. controls (post hoc analysis): $^{**}P < 0.01$; $^{***}P < 0.001$.
[†]Uterine weight (mg) as an index for sex steroid body impregnation. The minimum and maximum values for each group indicate the physiological range of hormone impregnation at time of euthenasia (n = 11–13/group). The uterine weights of controls were variable as expected for mice in different estrus cycles at the time of euthanasia. The uterine weights were decreased by 2-fold for placebo-treated EAE mice and by 2-fold for E2-treated EAE mice, indicating the effectiveness of estrogen administration (ANOVA followed by post hoc analysis, $F_{2,34} = 25.04$, $P < 0.0001$).
[‡]Plasma 17β-estradiol levels measured by immunoassay. $F_{2,18} = 96$, $P < 0.0001$.

Table S2. Relative levels of GFAP and CCL2 immunofluorescence in the different regions of the spinal cord in control (Con), EAE, and estrogen-treated EAE (EAE + E2) mice

	GFAP				
	Gray matter		White matter		
	Dorsal	Ventral	Dorsal	Ventral	Lateral
Con	100 ± 17	129 ± 8	71 ± 5	93 ± 6	97 ± 22
EAE	171 ± 17	177 ± 29	209 ± 28	270 ± 13*	263 ± 21*
EAE + E2	99 ± 11	121 ± 6	73 ± 2	152 ± 18	127 ± 8
P value	>0.05	>0.05	>0.05	0.027	0.049
	CCL2				
	Gray matter		White matter		
	Dorsal	Ventral	Dorsal	Ventral	Lateral
Con	100 ± 19	62 ± 6	39 ± 7	33 ± 2	29 ± 2
EAE	140 ± 9	99 ± 7	66 ± 3	92 ± 7*	42 ± 5*
EAE + E2	146 ± 22	90 ± 7	52 ± 14	57 ± 5	35 ± 2
P value	>0.05	>0.05	>0.05	0.027	0.047

Data are expressed as percentage of signal in control dorsal gray matter (n = 3 mice/group) with corresponding P values (Kruskal–Wallis, 3 mice/group). Dunn's post test analysis: *, $P < 0.05$ vs. Con.

Table S3. Estradiol treatment of EAE mice reduces immune cell infiltration as indicated by counts of CD45-immunoreactive cells in the white matter of EAE and estrogen-treated EAE (EAE + E2) mice

	dfu	vfu	lfu	Total
Con	0	1 or 2	0	1 or 2
EAE	29 ± 8	86 ± 9	220 ± 23	325 ± 37
EAE + E2	2.7 ± 1.3*	25 ± 5**	114 ± 17*	141 ± 18**

dfu, dorsal funiculus; lfu, lateral funiculi; vfu, ventral funiculus. Differences between EAE and estrogen-treated EAE mice are shown. t test: $^{*}P < 0.05$; $^{**}P < 0.01$.